Multi- to Unilamellar Transitions in Catanionic Vesicles

Patrizia Andreozzi,[†] Sergio S. Funari,[‡] Camillo La Mesa,*[,†,§] Paolo Mariani,[||] Maria Grazia Ortore,*[,||] Raffaele Sinibaldi,[||] and Francesco Spinozzi[||]

Department of Chemistry, Università La Sapienza, Rome, Italy, HASYLAB, Hamburg, Germany, SOFT-INFM, Università La Sapienza, Rome, Italy, and Department of SAIFET & CNISM, Università Politecnica delle Marche, Ancona, Italy

Received: January 16, 2010; Revised Manuscript Received: April 1, 2010

Sodium dodecylsulfate (SDS) and cetyltrimethylammonium bromide (CTAB) dispersed in aqueous solution form catanionic vesicles. Depending on composition, such vesicles show different net charge, stability, and interaction capability, indicative of the strong impact that catanionic systems may have in gene therapy and drug delivery technologies. To reveal the interplay among composition, net charge, sensitivity to temperature changes, vesicle size, and inner structure, a series of experiments on catanionic vesicles prepared at different SDS/CTAB mole ratios was performed. Dynamic light scattering, small-angle X-ray scattering, and ζ-potential experiments allow one to characterize an unexpected critical phenomenon at the nanoscale level. On heating, vesicles increase in size, but at a critical temperature an abrupt vesicle size reduction has been observed, together with a transition from multi- to a unilamellar state. The critical temperature regularly depends on the SDS/CTAB mole ratio. The unilamellar state obtained upon heating is retained for weeks. These phenomena suggest a new way to produce stable unilamellar vesicles with tunable size and charge.

Introduction

Lipids form different liquid crystalline phases, depending on composition and temperature. Upon dilution, solutions, and dispersions replace lamellar and other ordered mesophases.[1] Dispersions generally consist of single-walled or multilayered vesicles (also termed liposomes) and cubosomes.[2] Such particles are obtained upon dilution, sonication, or extrusion, while alternative procedures make use of salts, polymers, or surfactants.[3] A lot of drawbacks are met in the stabilization of lipid dispersions since, as a rule, lipid-based vesicles are unstable and reform the lamellar phases from which they are made of.

Efforts were recently made to find organized systems fulfilling the same performances as natural lipids, and synthetic surfactant species (quaternary ammonium salts, generally) were used for these purposes.[4] Unfortunately, most pure ionic surfactants show denaturing properties and are not safe for "in vivo" applications. Alternatively, mixtures of oppositely charged surfactants can be used, since they exhibit a phase behavior very similar to that occurring in lipids.[5] In particular, equimolar mixtures of oppositely charged surfactants, defined as "catanionic" systems, mimic the structure and phase behavior of swelling lipids.[6] Nonstoichiometric mixtures composed by such surfactants also show a rich polymorphic behavior at room temperature, with formation of micelles, vesicles, solids, and lyotropic mesophases. The concentration range pertinent to the formation of such systems can be as low as 0.1−1.0 wt %.[7] Catanionic mixtures are moderately cytotoxic and have been extensively used in studies dealing with protein uptake or DNA transfection.[8] This is why there has been so much interest toward such systems.

Accordingly, special attention has been devoted to rationalize the stability of selected catanionic mixtures, and to find rational strategies for getting unilamellar vesicles. However, the thermal stability and the presence of temperature-induced phase transitions have been rarely investigated. As a result of thermal motions, the bilayers of catanionic vesicles are expected to become progressively more fluid, to change their spontaneous curvature, and, eventually, to form new phases. Unfortunately, structural information and experimental evidence in this regard are poor and contradictory.[9] In this work, the catanionic system constituted by sodium dodecylsulfate (SDS) and cetyltrimethylammonium bromide (CTAB) has been investigated with different experimental techniques in order to determine the transitions from multi- to unilamellar states and to characterize the inner structure and size of catanionic vesicles as a function of both temperature and composition.

Experimental Section

A. Materials. High purity SDS and CTAB were obtained from Sigma. Purification was performed by dissolution in hot ethanol, filtration, and precipitation with cold acetone. The procedure was repeated twice, and the products were vacuum-dried at 70 °C. Determination of their critical micelle concentrations (cmc′s) and Krafft temperatures were used as purity criterion.[10] Conductivity water ($\chi \leq 10^{-7}\ \Omega^{-1}\ cm^{-1}$ at 25.0 °C), prepared by distillation in alkaline $KMnO_4$, was used. Ethanol and acetone (Sigma) were of synthetic grade.

Vesicular dispersions were prepared at different SDS/CTAB mole ratios, indicated as R in the following (R = [SDS]/[CTAB]). The overall surfactant content in the mixtures was always set to 6.0 mmol kg^{-1} (grossly 0.2 wt % of dry matter). R values ranging from 1.1 to 2.4 were obtained by mixing isomolar aqueous SDS and CTAB solutions at temperatures slightly higher than the CTAB Krafft point.[11] In this way, a "liquid state" of the surfactants alkyl

* Corresponding author. Address: Dept. Chemistry, "La Sapienza" University, P.le A. Moro 5, I-00185 Rome, Italy. Tel: +39-06-491694; +39-06-49913707. Fax: +39-06-490631. E-mail: camillo.lamesa@uniroma1.it (C.L.M.). Address: Dept. SAIFET, Università Politecnica delle Marche, Via Brecce Bianche, I-60131 Ancona, Italy. Tel. +39-071-2204664. Fax. +39.0712204605. E-mail: mg.ortore@alisf1.univpm.it (M.G.O.).

[†] Department of Chemistry, Università La Sapienza.

[‡] HASYLAB.

[§] SOFT-INFM, Università La Sapienza.

[||] Università Politecnica delle Marche.

10.1021/jp100437v
Published on Web 05/27/2010

chains is ensured. Upon mixing, vesicles are formed in seconds, as inferred by an abrupt increase in the overall mixture turbidity. No sedimentation, phase separation, or birefringence was observed, even after long-term equilibration. Note that equilibrium is reached after staying at room temperature for some days, and that no sonication is needed.

B. Dynamic Light Scattering (DLS). A Zeta Nanosizer unit, Malvern, was used to perform dynamic laser light scattering measurements at 632.8 nm. The instrument was operating in back scattering mode (BSM) at an angle of 173°, as such configuration allows performing measurements in turbid dispersions and minimizes multiple scattering effects. In addition, the instrumental facilities automatically determine the proper sample thickness to be investigated and focus the beam at a given position from the cell walls, depending on the system turbidity. In this way, some experimental drawbacks are overcome.

Quartz cells were cleaned by acid $K_2Cr_2O_7$ and washed several times with bidistilled water, until neutrality of the washing fluid was attained. Thereafter, the cells were dried by air flow. Measurements were run at least 5.0 min after introducing the sample in the scattering cell, to ensure the attainment of thermal equilibrium. The sample temperature was controlled to ±0.1 C° by a Peltier facility.

Correlation fits of the scattering intensity, reported as $I(t)$ versus log t plots, were elaborated by a CONTIN algorithm.[12] The temporal autocorrelation function was obtained; it was used to determine the apparent self-diffusion coefficient and, hence, the vesicles hydrodynamic diameter, D_H.[13] The errors on vesicles size inferred from the fits are some tens of nanometers, at most.

C. ζ-Potential. ζ-potential experiments, which provide information on the charge density of particles moving in an electric field,[14] were performed at 25.0 °C using a Malvern laser-Doppler unit and cells with gold-coated electrodes. The scattered light passing in the medium, when it is subjected to the effect of an applied electric field, undergoes a frequency shift compared to unperturbed conditions. Proper elaboration of the shift gives the particles electrophoretic mobility and the related ζ-potential value.

D. Transmission Electron Microscopy (TEM). The morphology of the catanionic vesicles was examined by TEM. Vesicular dispersions were first stratified onto copper grids, and the excess was removed by filter paper. Then, 2.0% phosphotungstic acid solution was stratified, and the acid in excess was removed. The sample was air-dried and then observed using a ZEISS EM900 electron microscope working at an accelerating voltage of 80 kV. Due to the dry conditions required in sample preparation, vesicle size and size distribution were considered only indicative.[15]

E. Small-Angle X-ray Scattering (SAXS). SAXS experiments were performed at the DESY synchrotron facility in Hamburg, Germany, on the A2 beamline. The investigated q-range ($q = 4\pi \sin\theta/\lambda$, where 2θ is the scattering angle and $\lambda = 1.50$ Å the X-ray wavelength) was 0.02−0.35 Å^{-1}. Experiments were run at 20.0 °C as a function of R, and as a function of temperature at an SDS/CTAB mole ratio of 1.71. Scattering data were recorded on a bidimensional CCD camera of 1024 × 1024 pixels, radially averaged and corrected for the dark, detector efficiency and sample transmission.[16] A few X-ray diffraction experiments were performed using a laboratory 3.5 kW Philips PW 1830 X-ray generator equipped with a Guinier-type focusing camera operating with a bent quartz crystal monochromator ($\lambda = 1.54$ Å). Diffraction patterns were recorded on GNR Analytical Instruments Imaging Plate system. Samples were held in a vacuum tight cylindrical cell provided with thin mylar windows. Diffraction data were collected at 25 °C.

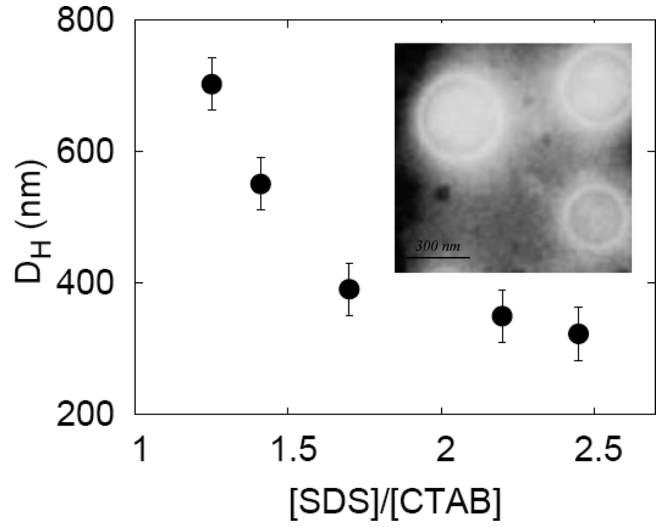

Figure 1. Composition dependence of the vesicle hydrodynamic diameter, D_H, as derived from DLS experiments performed at 25.0 °C. Inset: TEM image of an $R = 1.50$ vesicular sample, showing the presence of vesicles in the size range reported from DLS measurements.

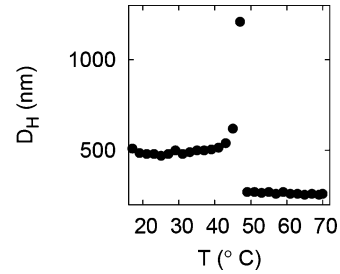

Figure 2. Temperature dependence of the vesicle average hydrodynamic diameter, D_H, derived from DLS experiments performed on a sample with $R = 1.71$. Error bars are within symbol sizes and have been calculated considering the polydispersion of D_H distributions.

Results and Discussion

A. DLS, TEM, and ζ-Potential. DLS experiments were performed at 25.0 °C as a function of vesicle composition. At first, it was derived that the average hydrodynamic diameter of vesicles, D_H, remains constant after sample equilibration. Second, the vesicle hydrodynamic diameter was observed to depend on composition, in full agreement with TEM observations (Figure 1). Composition effects are relevant: from data in Figure 1, it can be inferred that vesicle size diverges on approaching charge neutralization (i.e., D_H increases from 250 to 700 nm on decreasing R from 2.4 to 1.1). Hence, the residual charges located onto such vesicles play a pivotal role in controlling their interfacial curvature.

The vesicle size is significantly affected by temperature. As evidenced in Figure 2, a noticeable upward shift of D_H, followed by a strong and sudden decrease above a critical temperature T_C, is detected on heating. Three points should be considered. First, T_C scales regularly with the vesicle composition. As shown in Figure 3, higher content in SDS implies lower T_C values: this fact offers the possibility to modulate the thermal transitions depending on the requested purposes. Second, the scaling law controlling vesicle growth is the same for all the investigated samples, and follows a power-law in $(1 - T/T_C)$. Third, at the critical temperature, a significant change in sample turbidity is observed. Whatever the sample mole ratio, the dispersions are milky below T_C and bluish and/or slightly opalescent above it. Once heated above T_C, vesicles retain the latter character for weeks.

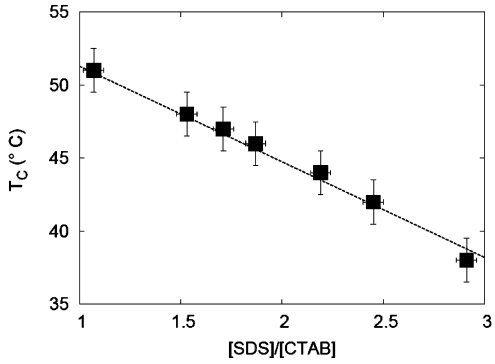

Figure 3. Composition dependence of the critical temperature, T_C (°C), on the [SDS/CTAB] mole ratio.

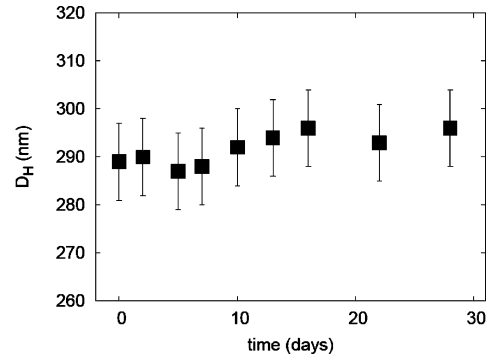

Figure 4. Time-dependence of vesicles average hydrodynamic diameter D_H. Data refer to the $R = 1.71$ mixture, equilibrated at 25.0 °C after a complete heating process up to 70 °C. Error bars have been obtained considering the variance of D_H distributions.

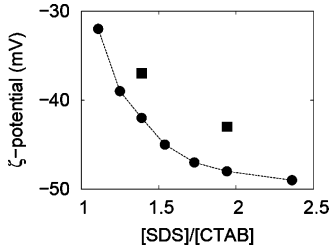

Figure 5. Composition dependence of the vesicle ζ-potential measured at 25.0 °C. Circles refer to equilibrium conditions and squares to freshly prepared samples. Error bars are smaller than symbol sizes. The line is only an eye-guide.

Constancy in vesicle size for long times is relevant for a possible use in biomedical applications. Therefore, DLS experiments were also performed as a function of time. As a main result, it was observed that, once the aforementioned heating cycles were completed, vesicles retain a nearly constant average hydrodynamic diameter for about 1 month. D_H values relative to the $R = 1.71$ sample, measured for over 1 month, are reported in Figure 4: it can be observed that D_H values range around 285−295 nm. In the investigated time frame, the drift is small, about 10−12 nm, and very comparable with the estimated experimental error bars.

Larger departures from the above trends are observed for longer times, particularly if samples are kept at temperatures well below 25 °C. Note that this is, approximately, the Krafft temperature of CTAB, at which the formation of a solid surfactant phase may occur. In such case, nucleation into multilamellar entities is counteracted by phase transition processes.

ζ-Potential results are finally reported in Figure 5. Data show that ζ-potential increases in absolute value on increasing R (i.e., moving away from the charge neutralization threshold). Moreover, differences between freshly prepared samples and those in equilibrium conditions occur. This behavior could be related to the time required to get true equilibrium conditions, according to a rearrangement of the surfactants into vesicles and/or to their partition between vesicles and the bulk.

B. SAXS. SAXS provides information on the inner structure of the vesicles at the nanoscale level.[17,18] At 20 °C and for all the investigated mole ratios (ranging from $R = 1.18$ to $R = 1.99$), the scattering curves are characterized by the occurrence of Bragg peaks (Figure 6, left frame), indicating the multilamellar nature of vesicles. Upon heating, the peaks disappear (see the right frame in the figure), suggesting a transition from multi- to unilamellar organization. As the above transition occurs at temperatures very close to that observed by DLS, it can be inferred that the strong decrease of D_H values above T_C is also associated with a transition from multi- to unilamellar vesicles. In other words, DLS refers to the modifications in the overall vesicle size, whereas SAXS refers to their inner organization; the two effects are strictly interrelated.

From the position of the Bragg peaks, the lamellar repeat distance, d, was determined. At 20 °C, d is around 37.5 Å, and shows no correlation with composition. Conversely, it slightly increases upon heating.

SAXS data obtained at temperatures below 50 °C were analyzed by model-dependent fitting procedures.[18,19] In particular, the intervesicle structure factor was set to unity, as the dispersions are diluted, and the multilamellar stacks were represented by the product of the form factor for infinite lamellae, $F(q)$, and the structure factor related to the bilayer stacking order, $S(q)$. Calculations were performed using the GENFIT software package.[19]

In particular, the X-ray scattering intensity was written as

$$I(q) = cS(q)[F(q)]^2/q^2$$

where c is a normalization factor, being the experimental data obtained in relative units.

The form factor is described as a Fourier transform of the electron density distribution normal to the bilayer plane, $\rho(z)$, determined considering the water, polar, and paraffinic layers to have thicknesses and electron densities of d_{wat}, d_{pol}, d_{par}, and ρ_{wat}, ρ_{pol}, ρ_{par}, respectively:

$$F(q) = \int_{-d/2}^{d/2} \rho(z) \cos(qz)\, dz$$

Referring to the bilayer model reported in Figure 7, it is evident that $d_{wat} = d - (2d_{pol} + d_{par})$. The water electron density has been fixed to $\rho_{wat} = 0.33$ e/Å^3, while d_{pol}, d_{par}, ρ_{pol}, and ρ_{par} have been treated as fitting parameters.

The structure factor $S(q)$ is related to the bilayer stacking order and has been modeled according to the modified Caillé theory.[20,21] This theory accounts for the number of strongly interacting bilayers, N, and for the respective undulation effects, which are measured by the so-called Caillé fluctuation parameter, η_1:

$$S(q) = N + \left\{ 2 \sum_{m=1}^{N-1} (N - m) \cos(mqd) \exp \times \left[-\left(\frac{d}{2\pi}\right)^2 q^2 \eta_1 \gamma \right] (\pi m)^{-(d/2\pi)^2 q^2 \eta_1} \right\}$$

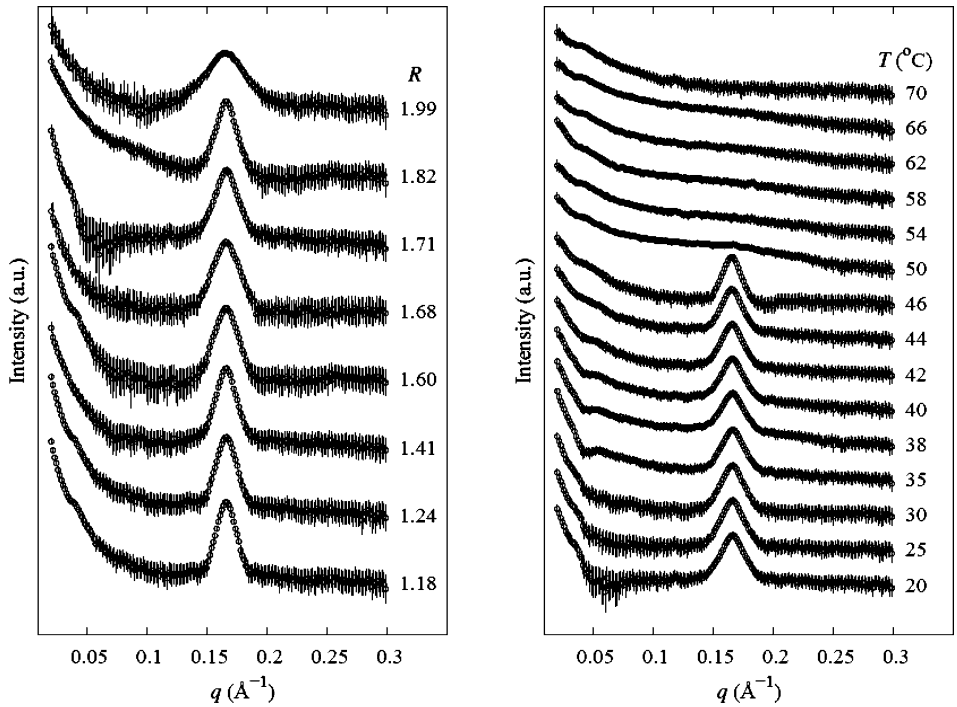

Figure 6. SAXS profiles obtained in different experimental conditions. Left frame: data obtained at $T = 20$ °C as a function of R, as indicated. Right frame: data obtained from a $R = 1.71$ vesicular sample as a function of temperature, as indicated.

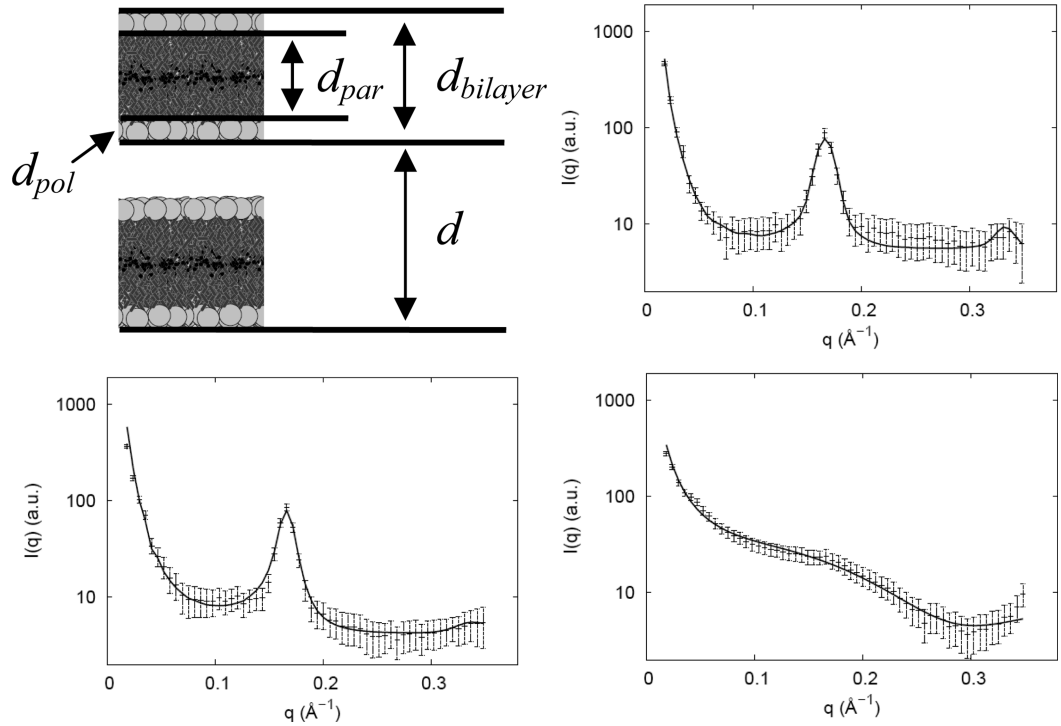

Figure 7. Top, left side: sketch of the bilayer model illustrating the structural parameters. Top, right frame: $R = 1.71$, $T = 20$ °C. Fitting parameters: $d_{pol} = 3.2$ Å, $d_{par} = 16.8$ Å, $\rho_{pol} = 0.382$ e/Å^3, $\rho_{par} = 0.281$ e/Å^3, $N = 7.4$, $\eta_1 = 0.029$. Bottom, left frame: $R = 1.71$, $T = 44$ °C. Fitting parameters: $d_{pol} = 3.9$ Å, $d_{par} = 24.9$ Å, $\rho_{pol} = 0.354$ e/Å^3, $\rho_{par} = 0.280$ e/Å^3, $N = 13.9$, $\eta_1 = 0.095$. Bottom, right frame: $R = 1.71$, $T = 50$ °C. Fitting parameters: $d_{pol} = 3.0$ Å, $d_{par} = 26.1$ Å, $\rho_{pol} = 0.371$ e/Å^3, $\rho_{par} = 0.278$ e/Å^3, $N = 1.4$, $\eta_1 = 0.29$.

where γ is the Euler's constant ($\gamma = 0.5772$). Note that the fluctuation parameter η_1 is related to the bending modulus of the bilayer, K_c, and to the bulk modulus for compression, B:

$$\eta_1 = \frac{\pi k_B T}{2d^2\sqrt{K_c B}}$$

Some significant fitting results are shown in Figure 7. The good capacity of the above model to reproduce the data is evident from the fit.

Data analysis shows that the thicknesses of polar and paraffinic layers, as well as the Caillé parameters, do not depend on R ($d_{pol} = 3.6 \pm 0.6$ Å, $d_{par} = 16.8 \pm 1.4$ Å, $\eta_1 = 0.037 \pm 0.009$, $N = 9.0 \pm 1.7$), with the exception of samples with $R =$

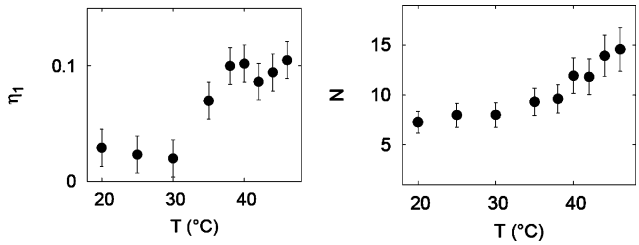

Figure 8. Temperature dependence of the Caillé fluctuation parameter, η_1 (left), and number of interacting bilayers, N (right), for the $R = 1.71$ sample.

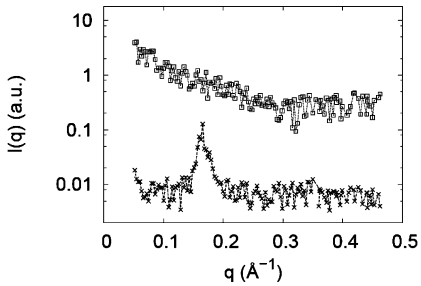

Figure 9. X-ray diffraction curves obtained from $R = 1.71$ vesicles, stored at 25 °C for 4 weeks, before the thermal cycle (bottom) and after the thermal cycle (top).

1.99, in which the computed number of interacting bilayers reduces to 3. Conversely, fitting parameters depend on temperature. The bilayer thickness increases on heating from 24 to 34 Å (at T_c), while d_{par} changes from ca. 17 to 26 Å. The stretching of hydrocarbon chains, coupled with a reduced interdigitation, can explain such a modification. Changes in η_1 and N are reported in Figure 8. Fluctuations in Caillé's theory are related to elastic deformations of the membrane stacks, and an increase in η_1 corresponds to a decrease in the product of the two elastic constants. On heating, the product $(K_cB)^{1/2}$ decreases from 15 to 4.8 erg cm^{-2}, indicating a significant softening of the lamellar stacking as a function of temperature. On the other side, the behavior of N with temperature (Figure 8), which does not explain by itself the large vesicle hydrodynamic diameter observed by DLS on heating, confirms vesicle growth and/or fusion before T_c is reached.

X-ray diffraction experiments have been also performed on vesicles stored for 4 weeks at 25 °C directly after preparation and after the previously mentioned thermal cycle. Two significative curves (both referring to $R = 1.71$ samples: a thermally cycled one and a not cycled one) are shown in Figure 9. Even if data are noisy, the observed profiles confirm that once the heating cycle was completed, vesicles retain the unilamellar character, while noncycled samples are still multilamellar (in this case, no changes not even in the unit cell parameter were detected).

Conclusions

The experimental results reported here indicate that changes in vesicle size are concomitant to variations in their inner structure. Upon heating, the vesicle state changes from a multi- to a unilamellar state, following vesicle fusion and growth mechanisms. Interestingly, the lamellar order vanishes at T_c and, simultaneously, vesicles size diverges, according to a scaling law.[22]

The transition from multi- to unilamellar vesicles is driven by the combination of entropic, osmotic, double-layer, and other terms. It is not easily to argue whether the same behavior holds for other lipid mixtures.[23] The mono- to multilayer transition, the backward process, is long on an experimental time-scale, since unilamellar vesicles, prepared at high temperatures, remain undisturbed for long times. Temperature, then, can be used to obtain unilamellar vesicular dispersions with a well-defined net charge. The above procedure could give rise to kinetically stable monolayer dispersions, to be used in many biomedical applications. Work along this line is promising. The procedures reported in this work could be also used when T values close to hyper-, or hypothermal conditions are dealt with. The optimization inherent to thermal conditioning requires a delicate balance between vesicle composition, osmotic forces, and working temperature. It can be fruitful in a lot of biomedically oriented applications.

Acknowledgment. We thank R. Muzzalupo, Università della Calabria, for TEM measurements. The research leading to these results has received funding from the European Community Seventh Framework Programme (FP7/2007-2013), under Grant Agreement No. 226716.

References and Notes

(1) Chernik, G. G. *Curr. Opin. Colloid Interface Sci.* **2000**, *4*, 381.
(2) Angelov, B.; Angelova, A.; Papahadjopoulos-Sternberg, B.; Lesieur, S.; Sadoc, J.-F.; Ollivon, M.; Couvreur, P. *J. Am. Chem. Soc.* **2006**, *128*, 5813.
(3) (a) Zepik, H. H.; Walde, P.; Ishikawa, T. *Angew. Chem., Int. Ed.* **2008**, *47*, 1323. (b) Esposito, E.; Cortesi, R.; Drechsler, M.; Paccamiccio, L.; Mariani, P.; Contado, C.; Stellin, E.; Menegatti, E.; Bonina, F.; Puglia, C. *Pharm. Res.* **2005**, *22*, 2163.
(4) Simberg, D.; Weisman, S.; Talmon, Y.; Barenholz, Y. *Crit. Rev. Ther. Drug Carrier Syst.* **2004**, *21*, 257.
(5) Mueller, M.; Hoffmann, H. In *Mixed Surfactant Systems*, 2nd ed.; von Wandrowszka, R., Ed.; Surfactant Science Series; M. Dekker: New York, 2005, Vol. 124; p 403.
(6) Marques, E. F.; Regev, O.; Khan, A.; Lindman, B. *Adv. Colloid Interface Sci.* **2003**, *100*, 83.
(7) Bonincontro, A.; Falivene, M.; La Mesa, C.; Risuleo, G.; Ruiz-Pena, M. *Langmuir* **2008**, *24*, 1973.
(8) Mel'nikov, S. M.; Dias, R.; Mel'nikova, Y. S.; Marques, E. F.; Miguel, M. G.; Lindman, B. *FEBS Lett.* **1999**, *453*, 113.
(9) Tondre, C.; Caillet, C. *Adv. Colloid Interface Sci.* **2001**, *115*, 134.
(10) Rico, I.; Lattes, A. *J. Phys. Chem.* **1986**, *90*, 5870.
(11) Letizia, C.; Andreozzi, P.; Scipioni, A.; La Mesa, C.; Bonincontro, A.; Spigone, E. *J. Phys. Chem. B* **2007**, *111*, 898.
(12) Zhou, Z.; Chu, B.; Nace, V. M.; Yang, Y.-W.; Booth, C. *Macromolecules* **1996**, *29*, 3663.
(13) Pusey, P. N.; Tough, R. J. A. In *Dynamic Light Scattering and Velocimetry*; Pecora, R., Ed.; Plenum: New York, 1981.
(14) Andreozzi, P.; La Mesa, C.; Masci, G.; Suber, L. *J. Phys. Chem. C* **2007**, *111*, 18004.
(15) Muzzalupo, R.; Tavano, L.; Trombino, S.; Cassano, R.; Picci, N.; La Mesa, C. *Colloids Surf. B: Biointerfaces* **2008**, *64* (2), 200.
(16) Sinibaldi, R.; Ortore, M. G.; Spinozzi, F.; Funari, S.; Teixeira, J.; Mariani, P. *Eur. Biophys. J.* **2008**, *37*, 673.
(17) (a) Cardini, G.; Baglioni, P.; Taddei, G. *Chem. Phys. Lett.* **1982**, *93*, 533. (b) Mariani, P.; Luzzati, V.; Delacroix, H. *J. Mol. Biol.* **1988**, *204*, 165.
(18) Spinozzi, F.; Carsughi, F.; Mariani, P.; Teixeira, C. V.; Amaral, L. *J. Appl. Crystallogr.* **2000**, *33*, 556.
(19) (a) Ortore, M. G.; Paciaroni, A.; Spinozzi, F.; Mariani, P.; Amenitsch, H.; Ollivier, J.; Barbosa, L. R. S.; Steinhart, M.; Russo, D. *J. R. Soc. Interface* **2009)** , *6*, S619–S634. (b) Barbosa, L. R. S.; Ortore, M. G.; Spinozzi, F.; Mariani, P.; Bernstorff, S.; Itri, R. *Biophys. J.*, in press.
(20) Zhang, R.; Suter, R. M.; Nagle, J. F. *Phys. Rev. E* **1994**, *50*, 5047.
(21) Frühwirth, T.; Fritz, G.; Freiberger, N.; Glatter, O. *J. Appl. Crystallogr.* **2004**, *37*, 703.
(22) Isojima, T.; Fujii, S.; Kubota, K.; Hamano, K. *J. Chem. Phys.* **2000**, *113*, 3916.
(23) Engelbrecht, J. R.; Mirollo, R. *Phys. Rev. E: Stat. Nonlinear Soft Matter Phys.* **2009**, *79*, 021904/1.

JP100437V